Membrane Conductance Analysis on Single-cell Electroporation with Electrolyte-filled Capillary

J. Anselmo [1], L. C. Ramos [1], J. L. B. Marques [1], F. R. M. B. Silva [2], and D. O. H. Suzuki [1]

[1] Institute of Biomedical Engineering, Department of Electrical Engineering
Federal University of Santa Catarina, Florianópolis, SC 88040-900, Brazil
suzuki@eel.ufsc.br

[2] Department of Biochemistry
Federal University of Santa Catarina, Florianópolis, SC 88040-900, Brazil

Abstract ─ Single-cell electroporation with electrolyte-filled capillary is a selective technique that affects the target cell without any consequences for the neighbouring cells. Inhomogeneous electric field caused by interaction of capillary, cell and environment in the experiment make the optimization setup difficult for DNA transfection efficiency. A electroporation model of membrane conductivity with experimental parameters was used to analyze the influence of cell-to-tip distance, cell-capillary dimensions relation, electrolyte and cytoplasm conductivity, and strength of the pulses on electroporation. Simulation results demonstrate that the nonlinear electric field distribution on cell membrane depends on tip-to-cell distance and may be the cause of cell survival. The electroporation with capillary are affected by the external medium, relation between the cell and capillary radius, tip-to-cell distance, and strength of the applied potential.

Index Terms ─ Electrolyte-filled capillary, electroporation, electroporation model, membrane conductivity, single cell.

I. INTRODUCTION

Electroporation or electropermeabilization is a phenomenon that occurs when high electric field is applied to increase the cell membrane permeability [1, 2].

The main applications of electroporation are electrochemotherapy [3], [4] and genetic manipulation [5]. The electroporation traditional methods to genetic transference use large, planar electrodes to produce a uniform electric field. However, some experimental cases investigate the response of a single cell, such as brain tissue and primary cultures [6], [7]. These cells present problems to DNA transfection. They tend to be very sensitive to physical stress alteration in temperature, ph shifts and changes in osmolarity. The strengths of single cell electroporations are surviving cells are completely functional; subsequent transfection of the same neuron with more than one construct at different time points; neurons up to 1 mm deep into a tissue can be transfected [8]; no need for vector or cytotoxic carriers [9]. The great disadvantages of single cell electroporation is the difficult of optimization [8], demands experimenter skill, laborious procedure [9].

The efficiency of this technique depends of interaction of environment (cell size and geometry, internal and external conductivity), capillary (cell-to-tip distance, capillary diameter) and electric field (strength and duration electric pulse). Some works proposed relations among parameters to improve the electroporation efficiency [2], [10]. These studies provide understanding about mechanical and electrical aspects of electroporation in cell membrane. It increases the gene transfer efficiency and viability of cells.

The inhomogeneous electric field caused by capillary and complex geometries in the experiment make the optimization setup difficult for the electroporation efficiency. The cell-to-tip distance and cell size affect the electroporation success rate and cell viability [6-8]. Each cell needs electroporation protocols in specific micropipette according to their characteristics.

In this study, a membrane conductivity model based on Glaser *et al.* [11] with electroporation parameters from cell suspension experiments [12] is implemented. This electroporation model was applied to study the effect of cell-to-tip distance, cell-capillary dimensions relation, electrolyte and cytoplasm conductivity, and strength of the pulses. The consequences of electric field distribution on membrane conductivity and current density through the membrane cell are analyzed. We start the elucidation of the physical and electrical influences of single cell electroporation to improve the efficiency of DNA transfection.

Submitted On: August 13, 2015
Accepted On: May 17, 2016

II. MATERIALS AND METHODS

A. Numerical and geometry modeling

The simulations in this study were performed using the COMSOL Multiphysics® software package (COMSOL Inc., Burlington, MA) based on the finite-element method.

The electric field distribution models were calculated using the steady current module. If the electric current density $\boldsymbol{J}$ in tissue is divergence-free, the solved equation is Poisson's equation:

$$-\nabla \cdot (\sigma \nabla V) = 0, \quad (1)$$

where σ is the conductivity (S/m) and V is the electric potential (V).

The processing was performed on a PC equipped with AMD Athlon™ II X2 250 3.0 GHz processor and 4.0 GB RAM. The computer was operating on a Microsoft® Windows 8 de 64 bits platform.

The geometrical model was simulated with a capillary perpendicular to the dish surface (Fig. 1). The full capillary length L_{cap} is 1.5×10^{-2} m, and extremely thin membranes (5×10^{-9}m) are problematic in meshing and solving the problem.

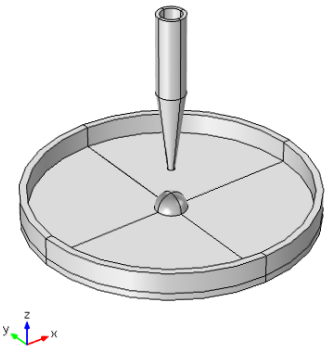

Fig. 1. Schematic representation of single-cell electroporation geometry. Components are not drawn to scale.

The solution was simulated by only 2×10^{-3} m of the pulled capillary. The cell and capillary are placed in the centred axis of simulation region for axial symmetry. The potential drop in the unpulled capillary is given by [13]:

$$V_a = V_{cap} + \frac{\partial V}{\partial z}(L_{cap} - l), \quad (2)$$

where $(\partial V/\partial z)$ is the electric field normal to the boundary where V_a exists, V_{cap} is the potential applied across L_{cap}, and l is the pulled tip length.

The boundary conditions and geometry simulated a represented in Fig. 2 and Table 1. A grid independence study was performed to establish an optimized mesh. Extremely fine mesh was set on the cell membrane and fine mesh in other geometries. The total mesh was 61,730 tetrahedral elements.

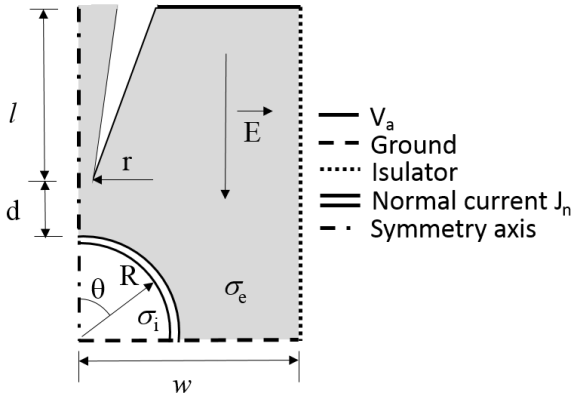

Fig. 2. Isolated single-cell model under nonlinear electric field. The capillary is positioned perpendicular to the Petri dish. The axisymmetry is used to reduce the computational resources.

Table 1: Units and corresponding symbols

Parameter	Symbol	Value
External conductivity [13]	σ_e	$0.60\ S/m$
Internal conductivity [13]	σ_i	$0.13\ S/m$
Cell radius	R	$10\times10^{-6}\ m$
Membrane thickness [12]	h	$5\times10^{-9}\ m$
Length of pulled tip	l	$2\times10^{-3}\ m$
Internal diameter unpulled capillary	D_i	$100\times10^{-6}\ m$
Internal diameter pulled capillary	r	$2.5\times10^{-6}\ m$

B. Electroporation model

The ionic transport across the pores formed on the electroporated membrane increase membrane conductivity. Assuming that the intact lipid matrix has a negligible ionic mobility, all ionic transports should happen through the pores. Glaser's experiments [11] suggest that the ionic mobility in an electroporated membrane increases with the rate depending on the transmembrane voltage. The electroporated membrane conductivity can be calculated by:

$$\frac{d\sigma_m}{dt} = Ke^{\left(\frac{V_m}{V_{pp}}\right)^2}, \quad (3)$$

where K is a electroporation constant and V_{pp} sets the critical transmembrane potential at which the membrane breaks down. This expression agrees with Glaser's model and experimental results.

The electroporation is a threshold phenomenon: when the induced transmembrane potential exceeds a critical value V_{pp}, there is pores formation on the membrane. The critical transmembrane potential is 0.2 V [14]. The K parameter was obtained by comparing the point at 100 μs of experimental and numerical suspension conductivity

during electroporation pulse [12] and simulation of single cell in a uniform electric field.

In this simulation, an increase in the suspension concentration is incorporated as a reduction in the correction factor on the local electric field around the cells [15]:

$$E_f = \frac{1+p/2}{1+(3p/4N\pi)^{1/3}} E, \quad (4)$$

where N is the arrangement type of cells and p is the volume fraction occupied by the cell.

The simulation took into account Equation (4) on the electric properties of cell membrane. Electric field distribution models were calculated using the steady current module as in Equation (1). The boundary conditions, electric and geometric parameters for these simulations are in Fig. 3 and Table 2.

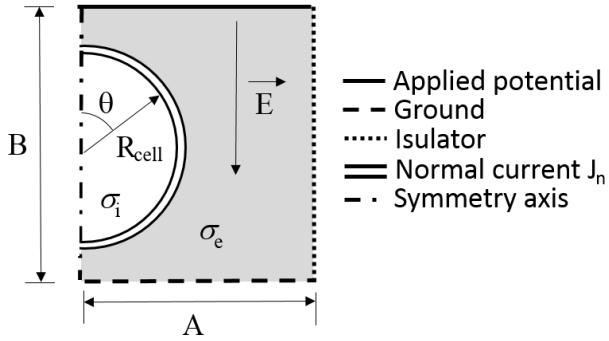

Fig. 3. Schematic of a spherical cell of radius R_{cell} in a uniform electric field. Arrow indicates the direction of the electric field E, polar angle θ measures the position along the cell circumference. The axial-symmetry geometry and boundary conditions are presented.

Table 2: Units and corresponding symbols

Definition	Symbol	Value
Electroporation constant	K	$3\times10^{-2}\ S/m.s$
Critical transmembrane potential [14]	V_{pp}	$0.20\ V$
Cell radius[12]	R_{cell}	$4.87\times10^{-6}\ m$
External conductivity [12]	σ_e	$0.55\ S/m$
Internal conductivity [12]	σ_i	$1.0\ S/m$
Arrangement type of cells [12]	N	4
volume fraction of cells [12]	p	0.28
Simulation width	B	1×10^{-3}m
Simulation height	A	0.5×10^{-3}m

III. RESULTS

Comparing the experimental and theoretical results of cell suspension conductivity, the parameter $K = 3.10^{-2}$S/m. s is obtained for $V_m(\sigma_m = 0)$ between 1.8 V and 3.3 V. The errors between the theoretical and experimental curves account for less than 15% as shown in Table 3.

The transmembrane potential increases according to Equation (1): when V_m exceeds a critical value (V_{pp}), there are the creations of pores and σ_m increases. The angular distributions of membrane conductivity and transmembrane potential are strongly dependent on the distance between cell membrane and capillary (d) as shown in Fig. 4, electric potential applied are 500 V and 1000 V. The maximum values of σ_m were near the pole. The simulation was performed with parameters from Table 1, the electroporation phenomena was modeled by Equation (3) with $K = 3.10^{-2}$ S/s and $V_{pp} = 0.20\ V$.

Table 3: Comparing of Ramos *et al*. [12] experiments and electroporation model of Equation (3)

$V_m(\sigma_m=0)$ (V)	Ref. [10]* (S/m)	Model (S/m)	Error %
1.8	6.5×10^{-6}	5.9×10^{-6}	9.8
2.2	9.0×10^{-6}	7.7×10^{-6}	14.2
2.6	1.2×10^{-5}	1.1×10^{-5}	10.3
2.9	1.3×10^{-5}	1.5×10^{-5}	11.1
3.3	2.0×10^{-5}	2.1×10^{-5}	6.0

*$\sigma_m = h.G_m$ [29].

Figure 5 presents the electric field distribution between capillary and cell membrane, d = 0.5 µm, and applied potential of 500 V and 1000 V. The lines represent the current density during the electroporation.

Dynamics of transmembrane potential induced and membrane conductance for different applied potentials through the capillary are shown in Fig. 6.

Figure 7 shows the influence of cell geometry on the electroporation with capillary near the cell. The transmembrane potential did not differ significantly when the cell radius is over 20 µm. The effects of internal and external conductivity are analyzed in Figs. 8 and 9. The conductivities values and cell radii of the simulations are limited to biological parameters [16].

IV. DISCUSSION

Based on Glaser's experiments [11], we propose that the membrane conductivity increases with the rate depending on the transmembrane voltage, Equation (3). The critical membrane potential proposed by Glaser is 0.46 V. However this potential was obtained with experiments with lipid bilayer. The experiments with different cells conclude that $V_{pp} = 0.2$ V [14]. These results are suitable for our experiments, because the K value was obtained from experiments with cell suspensions [12]. This parameter has different values when compared with the literature [2, 11, 15]. The difficulty in comparing the K value is caused by different

parameters measured between experiments. Glaser *et al.* [11] fit the current results with the electroporation model of Equation (3). Suzuki *et al.* [2] investigated the conductivity of cell suspensions when compared with two electroporation models. Although a variation was expected in these values, the dynamics of the model is consistent with different experiments. The results obtained with our findings and literature experiments support the model at the beginning of the electroporation processes.

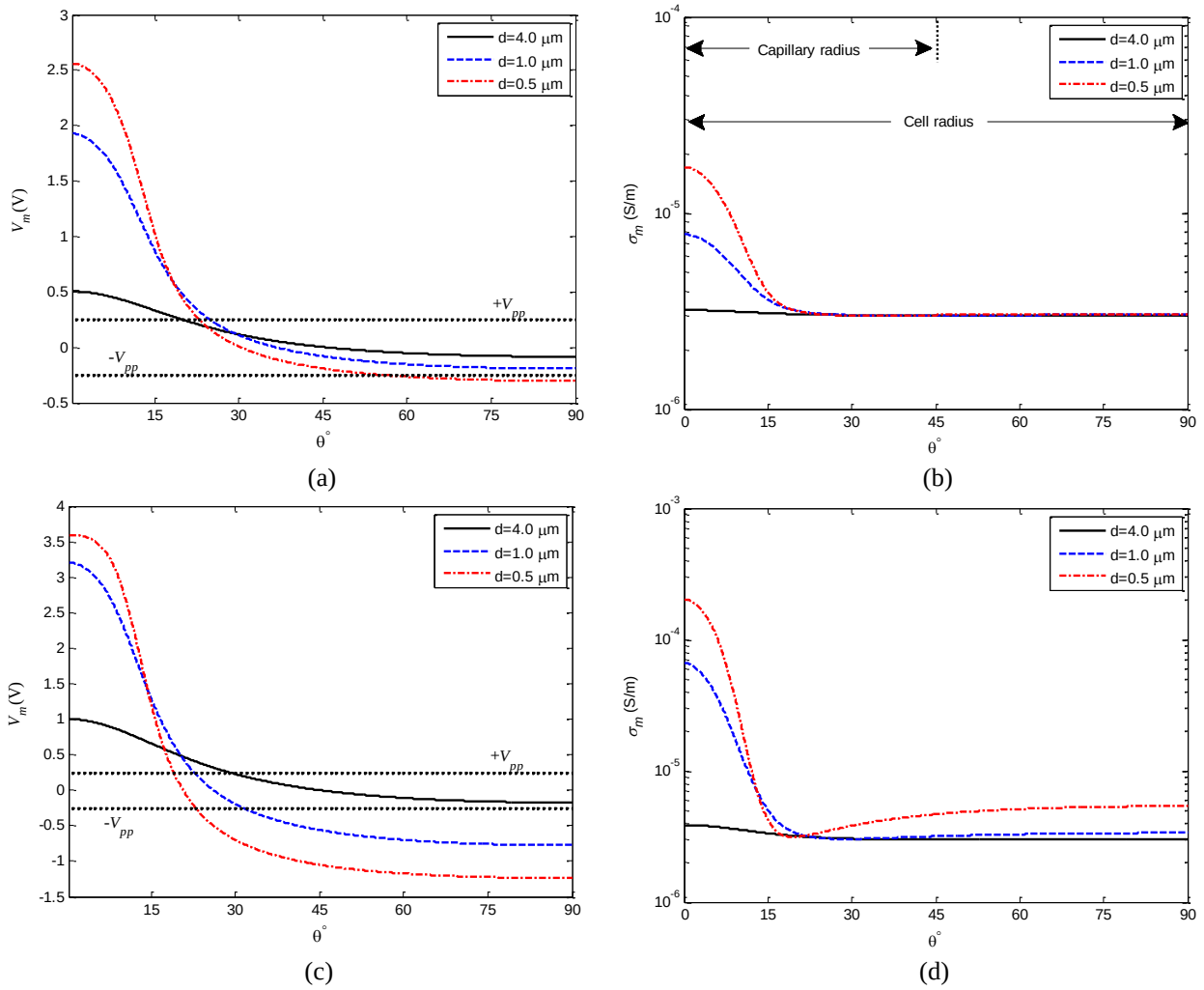

Fig. 4. Angular distribution of transmembrane potential and electroporated membrane conductivity, respectively, for applied electric potential (a) and (c) 500V, (b) and (d) 1000V. (d) Is the distance between capillary and cell membrane (tip-to-cell). Dashed parallel lines mark threshold electroporation potential V_{pp}=0.2 V [14]. Cell radius of 10 μm, electroporation model on the Equation (3) at steady state, σ_o=0.60 S/m and σ_i=0.13 S/m.

Our findings are consistent with the previous reports of membrane conductance indicating that the electroporation model and the geometric implementation of the model are consistent for these studies [16-20]. In this work, the intact membrane conductance is neglected. The σ_m with 500 V and d=4×10^{-6} m is about 3×10^{-6} S/m as shown in Fig. 4 (b). This value can be considered insignificant because it does not cause reduction of transmembrane potential. The comparison between V_m curve in Fig. 4 (a), d=4×10^{-6} m, and Zudans *et al.* (Fig. 9 from [13]) present less than 2% error. Some experimental and theoretical work estimated the electroporated membrane conductivity (σ_m= $h.G_m$ [17]) at about 10^{-4} S/m [2], [18]. However, Hibino *et al.* [19] presented estimated values in the range from 10^{-4} S/m to 5×10^{-4} S/m. Pavlin *et al.* [20], [21] showed theoretical studies of effective conductivity of a suspension of cells, using σ_m=4×10^{-4} S/m. Kinosita and Tsong [22], [23] presented values on erythrocytes between σ_m=5×10^{-4} and 5×10^{-3} S/m. The results in Figs. 4 (b) and 4 (c) confirm the previous results.

The σ_m and V_m variation is higher on polar angle as

shown in Figs. 4 and 6. The reduction of distance between the capillary and the membrane increases the transmembrane potential and, consequently, σ_m.

The applied potential of 500 V produces opened pores on the membrane between 0° and 20° (Fig. 4 (b)). It happens because the outer to inner face of the cell membrane is over threshold potential. This area is smaller than the capillary radius. For 1000 V, σ_m increases until 20°. However, over 20°, the pores are created because there is a $V_m > V_{pp}$ from inner to outer face of the cell membrane as shown in Fig. 4 (d). It is of interest to note that most ionic current flows from the capillary to the cytoplasm through the electropores (solid lines in Fig. 5). However, over 20° there is a small current that flow out from the cell. It is insignificant when compared with the current on the pole cell.

The temporal dynamic of electroporation are presented in Fig. 6 with different electric fields. After the applied potential, V_m increases. When the threshold potential is over 200 mV, there is a quick increase in σ_m, the pores are created and the ions flow across the cell membrane. These ionic fluxes through the membrane reduce the V_m and stabilize σ_m, as shown in Fig. 6 (b). After the initial electroporation process, there is equilibrium between V_m and ion diffusion through the electropores.

The relation between the cell and capillary radius (R/r) is associated with the electroporated membrane conductivity and pore opened as shown in Figs. 7 and 8. The electroporation effect is not effective when cell radius is smaller than the capillary radius (*e.g.*, bacteria). However, the electroporation with capillary presents optimization results if cell dimensions are twice the capillary diameter. The transport of molecules and DNA using this technique is adequate for adherent cells and tissues (*in vivo*) as CHO and WSS Cells [24] and brain tissue [25], because the cell dimensions are bigger than those of the capillary. Agarwal *et al.* [26] presented experimental and numerical evidences of the cell size dependence on electroporation effect with the capillary as shown in Fig. 7.

The proximity of cell and capillarity is 0.5×10^{-6} m when R/r is over 4 and it produces localized high transmembrane potential ($\theta<15°$). This effect happens because the cell membrane is almost plane in relation to the capillary.

An important factor for efficiency on electroporation is the cell survival. This parameter is associated with a fraction of the electroporated area [26]. In cell suspension, the cell survival is related with pulse amplitude [1]. The pulse amplitude is not suitable for the available cell survival with capillary. The applied electric field is not uniform and the transmembrane potential without electroporation is not available from Equation (1), Figs. 4 (a) and 4 (c). The cell survival on electroporation is related to the ions efflux into cell. This ionic imbalance and swelling can provide the death of the cell [27]. Figure 4 (d), $d=0.5\times10^{-6}$ m, presents an extensive electroporated area in relation to total membrane area. The simulation provides information that the applied electric pulses of 1000 V, $d=0.5\times10^{-6}$ m, and cell radius of 10×10^{-6} m can kill the cells.

Figures 8 and 9 show that the membrane conductivity is higher when the external medium increases. Some experiments with electroporation present low conductivity medium ($\sigma_o<0.2$ S/m) [21], [26]. Our model prediction provides results that these media can decrease the membrane conductivity. However, there is no consensus about any direct relation between membrane conductivity and molecular uptake to cells. Sadik *et al.* [28] describe a decrease of molecule diffusion with increase in medium conductivity. The physical mechanism underlying diffusion through the electropores is not completely understood.

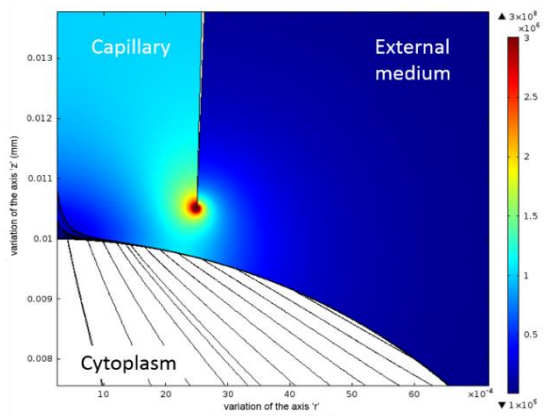

(a)

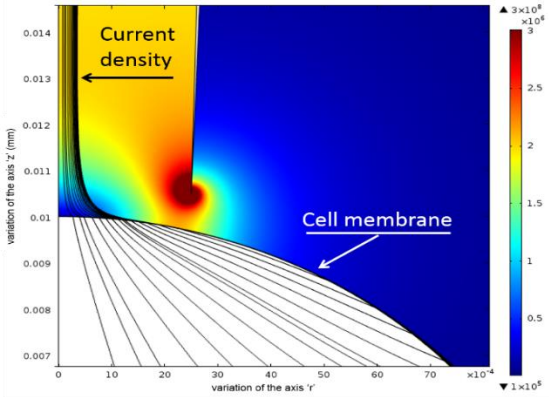

(b)

Fig. 5. Electric field distribution with distance between capillary and membrane cell of 0.5 μm. The lines represent current density components. (a) 500 V and (b) 1000 V. The color bar unit is V/m. The electropores are concentrated on the pole cell where the current lines are intense.

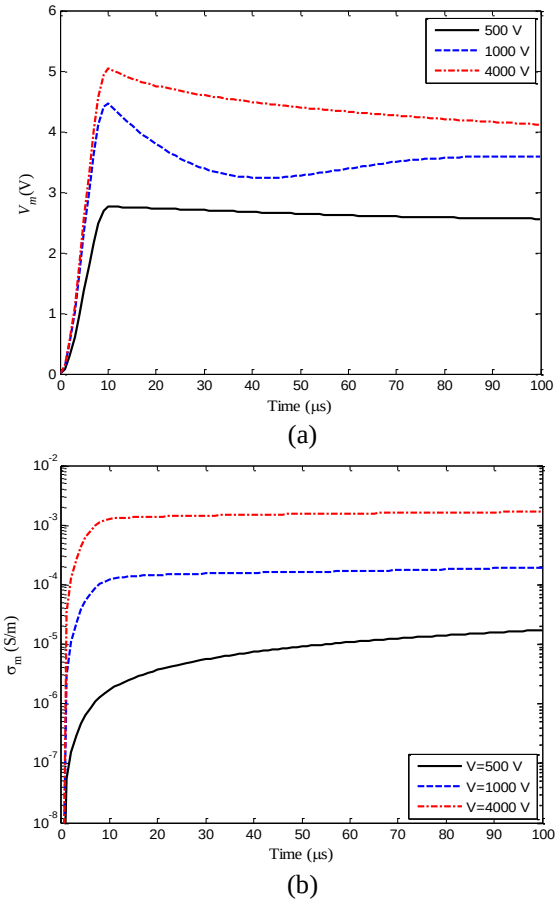

Fig. 6. Simulation of different applied potentials through the capillary on cell membrane with d=0.5 μm. (a) Transmembrane potential and (b) membrane conductance on the cell pole for different applied potentials. The cell radius is 10 μm.

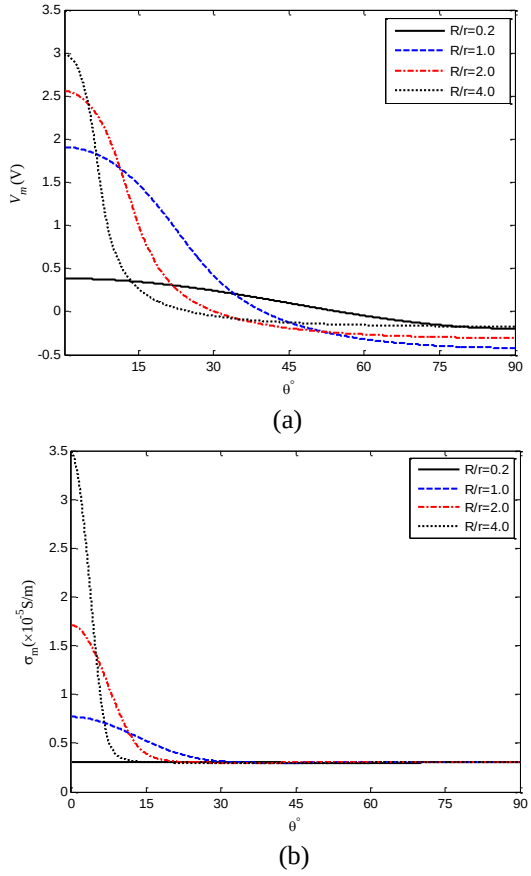

Fig. 7. Effect of relation between cell and capillary radius (*R/r*) on (a) transmembrane potential and (b) membrane conductivity at steady state. Distance between capillary and cell membrane is d=0.5×10^{-6} m, applied potential is 500V, σ_o=0.60 S/m and σ_i=0.13 S/m. The capillary radius is 5×10^{-6} m.

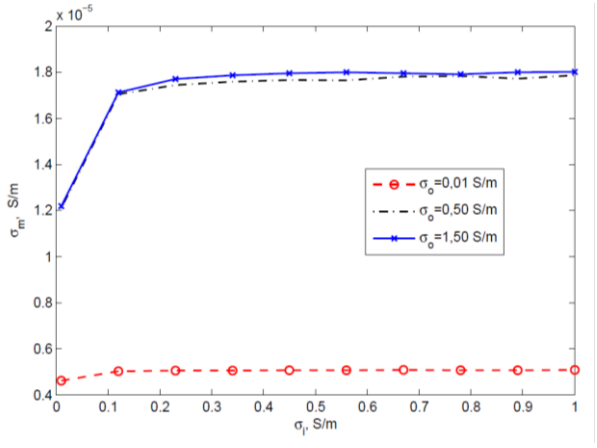

Fig. 8. Relation of membrane conductivity and internal conductivity for three external conductivity. Applied potential is 500V and d= 0.5μm. The capillary radius is 5×10^{-6} m.

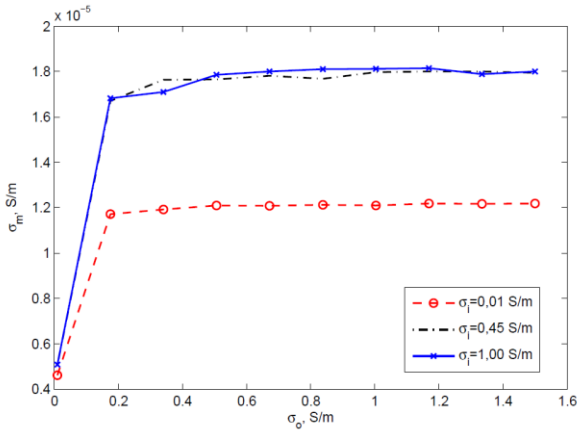

Fig. 9. Effect of external conductivity on membrane conductance for three internal conductivity. Applied potential is 500V and d= 0.5μm. The capillary radius is 5×10^{-6} m.

V. CONCLUSION

This study proposed an electroporation model based on Glaser *et al*. theories and Ramos *et al*. experiments. The membrane conductivity results are similar to previous works.

The high electric potential applied through capillary presented non linear electric field distribution on cell membrane (Figs. 4 (a), 4 (c) and 5). This effect may be reduced the cell survival.

The important factors that affect the electroporation with capillary are: external medium; relation between cell and capillary radius; distance between capillary; and membrane and strength applied potential.

ACKNOWLEDGMENT

The authors acknowledge financial support from CNPq, Brazilian researches funding agency (CNPq 477443/2012-5).

REFERENCES

[1] T. Kotnik, P. Gorazd, and D. Miklavcic, *The Cell in the Electric Field*, in Clinical Aspects of Electroporation, J. G. Stephen, T. Kee, and E. W. Lee, Ed. New York, NY: Springer Science+Business Media, pp. 19-29, 2011.

[2] D. O. H. Suzuki, A. Ramos, M. C. M. Ribeiro, L. H. Cazarolli, F. R. M. B. Silva, L. D. Leite, and J. L. B. Marques, "Theoretical and experimental analysis of electroporated membrane conductance in cell suspension," *IEEE Trans. Biomed. Eng.*, vol. 58, no. 12, pp. 3310-8, Dec. 2011.

[3] D. O. H. Suzuki, J. Anselmo, K. D. de Oliveira, J. O. Freytag, M. M. M. Rangel, J. L. B. Marques, and A. Ramos, "Numerical model of dog mast cell tumor treated by electrochemotherapy," *Artif. Organs*, vol. in press, Jul. 2015.

[4] L. M. Mir, L. F. Glass, G. Sersa, J. Teissie, C. Domenge, D. Miklavcic, M. J. Jaroszeski, S. Orlowski, D. S. Reintgen, and Z. Rudolf, "Effective treatment of cutaneous and subcutaneous malignant tumours by electrochemotherapy," *Br. J. Cancer*, vol. 77, no. 12, p. 2336, 1998.

[5] P. A. Beare, K. M. Sandoz, A. Omsland, D. D. Rockey, and R. A. Heinzen, "Advances in genetic manipulation of obligate intracellular bacterial pathogens," *Front. Microbiol.*, vol. 2, no. May, p. 97, Jan. 2011.

[6] M. Wang, O. Orwar, J. Olofsson, and S. G. Weber, "Single-cell electroporation," *Anal. Bioanal. Chem.*, vol. 397, no. 8, pp. 3235-3248, 2010.

[7] K. Baek, C. Tu, J. Zoldan, and L. J. Suggs, "Gene transfection for stem cell therapy," *Curr. Stem Cell Reports*, pp. 52-61, 2016.

[8] D. Karra and R. Dahm, "Transfection techniques for neuronal cells," *J. Neurosci.*, vol. 30, no. 18, pp. 6171-6177, 2010.

[9] T. K. Kim and J. H. Eberwine, "Mammalian cell transfection: The present and the future," *Anal. Bioanal. Chem.*, vol. 397, no. 8, pp. 3173-3178, 2010.

[10] J. Li, W. Tan, M. Yu, and H. Lin, "The effect of extracellular conductivity on electroporation-mediated molecular delivery," *Biochim. Biophys. Acta - Biomembr.*, vol. 1828, no. 2, pp. 461-470, 2013.

[11] R. W. Glaser, S. L. Leikin, L. V Chernomordik, V. F. Pastushenko, and A. I. Sokirko, "Reversible electrical breakdown of lipid bilayers: formation and evolution of pores," *Biochim. Biophys. Acta (BBA)-Biomembranes*, vol. 940, no. 2, pp. 275-287, 1988.

[12] A. Ramos, A. L. S. Schneider, D. O. H. Suzuki, and J. L. B. Marques, "Sinusoidal signal analysis of electroporation in biological cells," *IEEE Trans. Biomed. Eng.*, vol. 59, no. 10, pp. 2965-73, Oct. 2012.

[13] I. Zudans, A. Agarwal, O. Orwar, and S. G. Weber, "Numerical calculations of single-cell electroporation with an electrolyte-filled capillary," *Biophys. J.*, vol. 92, no. 10, pp. 3696-705, May 2007.

[14] J. Teissié and M. P. Rols, "An experimental evaluation of the critical potential difference inducing cell membrane electropermeabilization," *Biophys. J.*, vol. 65, no. 1, pp. 409-413, 1993.

[15] Y. Qin, S. Lai, Y. Jiang, T. Yang, and J. Wang, "Transmembrane voltage induced on a cell membrane in suspensions exposed to an alternating field: A theoretical analysis," *Bioelectrochemistry*, vol. 67, no. 1, pp. 57-65, 2005.

[16] "Sensitivity of transmembrane voltage induced by applied electric fields – A theoretical analysis.pdf."

[17] W. M. Arnold, R. K. Schmutzler, A. G. Schmutzler, H. van der Ven, S. Al-Hasani, D. Krebs, and U. Zimmermann, "Electro-rotation of mouse oocytes: single-cell measurements of zona-intact and zona-free cells and of the isolated zona pellucida," *Biochim. Biophys. Acta (BBA)-Biomembranes*, vol. 905, no. 2, pp. 454-464, 1987.

[18] M. Schmeer, T. Seipp, U. Pliquett, S. Kakorin, and E. Neumann, "Mechanism for the conductivity changes caused by membrane electroporation of CHO cell-pellets," *Phys. Chem. Chem. Phys.*, vol. 6, no. 24, pp. 5564-5574, 2004.

[19] M. Hibino, H. Itoh, and K. Kinosita Jr., "Time courses of cell electroporation as revealed by submicrosecond imaging of transmembrane potential," *Biophys. J.*, vol. 64, no. 6, pp. 1789-1800, 1993.

[20] M. Pavlin and D. Miklavčič, "Effective conductivity of a suspension of permeabilized cells: a theoretical analysis," *Biophys. J.*, vol. 85, no. 2, pp. 719-729, 2003.

[21] M. Pavlin, M. Kandušer, M. Reberšek, G. Pucihar, F. X. Hart, D. Miklavčič, et al., "Effect of cell electroporation on the conductivity of a cell suspension," *Biophys. J.*, vol. 88, no. 6, pp. 4378-4390, 2005.
[22] K. Kinosita Jr. and T. Y. Tsong, "Voltage-induced pore formation and hemolysis of human erythrocytes," *Biochim. Biophys. Acta (BBA)-Biomembranes*, vol. 471, no. 2, pp. 227-242, 1977.
[23] K. Kinosita Jr. and T. Y. Tsong, "Voltage-induced conductance in human erythrocyte membranes," *Biochim. Biophys. Acta (BBA)-Biomembranes*, vol. 554, no. 2, pp. 479-497, 1979.
[24] J. Olofsson, M. Levin, A. Strömberg, S. G. Weber, F. Ryttsén, and O. Orwar, "Scanning electroporation of selected areas of adherent cell cultures," *Anal. Chem.*, vol. 79, no. 12, pp. 4410-4418, 2007.
[25] K. Nolkrantz, C. Farre, A. Brederlau, R. I. D. Karlsson, C. Brennan, P. S. Eriksson, S. G. Weber, M. Sandberg, and O. Orwar, "Electroporation of single cells and tissues with an electrolyte-filled capillary," *Anal. Chem.*, vol. 73, no. 18, pp. 4469-4477, 2001.
[26] A. Agarwal, I. Zudans, E. A. Weber, J. Olofsson, O. Orwar, and S. G. Weber, "Effect of cell size and shape on single-cell electroporation," *Anal. Chem.*, vol. 79, no. 10, pp. 3589-3596, 2007.
[27] S. Haberl, D. Miklavcic, G. Sersa, W. Frey, and B. Rubinsky, "Cell membrane electroporation-Part 2: the applications," *IEEE Electr. Insul. Mag.*, vol. 29, no. 1, pp. 29-37, Jan. 2013.
[28] M. M. Sadik, J. Li, J. W. Shan, D. I. Shreiber, and H. Lin, "Quantification of propidium iodide delivery using millisecond electric pulses: Experiments," *Biochim. Biophys. Acta (BBA)-Biomembranes*, vol. 1828, no. 4, pp. 1322-1328, 2013.
[29] W. M. Arnold, R. K. Schmutzler, A. G. Schmutzler, H. van der Ven, S. Al-Hasani, D. Krebs, and U. Zimmermann, "Electro-rotation of mouse oocytes: Single-cell measurements of zona-intact and zona-free cells and of the isolated zona pellucida," *Biochim. Biophys. Acta*, vol. 905, pp. 454-464, 1987.

Jânio Anselmo received a graduate degree in Electrical Engineering in 2011 from the University of Southern Santa Catarina (UNISUL), Florianópolis-SC, Brazil. He is currently an M.Sc. Student in Biomedical Engineering program at the Graduate in Electrical Engineering from the Federal University of Santa Catarina (UFSC-PGEEL). His research interests include modeling of biological processes through the phenomenon of electroporation.

Luciana Costa Ramos received a graduate degree in Electrical Engineering in 1996 from the Federal Technological University of Paraná (UTFPR), Curitiba-PR, Brazil. She is currently a M.Sc. Student in Biomedical Engineering program at the Graduate in Electrical Engineering from the Federal University of Santa Catarina (UFSC-PGEEL). Her research interests include modeling of biological processes through the phenomenon of electroporation.

Fátima R.M. B. Silva received the graduate degree in Chemistry from the Catholic University of Pelotas, Pelotas-RS, Brazil, in 1984, and the Ph.D. degree in Biochemistry from the Federal University of Rio Grande do Sul, Porto Alegre, SC, Brazil, in 1995. Since 1994, she has been researching and teaching as an Associate Professor at the Federal University of Santa Catarina. Her current interests include endocrine, physiology, and biochemical alterations in cells.

Jefferson L. B. Marques (M'02) received a graduate degree in Electrical Engineering in 1985 from the Federal University of Santa Maria, Santa Maria-RS, Brazil, and a Ph.D. degree in Medical Physics and Clinical Engineering in 1994 from the University of Sheffield, Sheffield, UK. He is currently an Associate Professor at the Federal University of Santa Catarina. His research interests include modeling of physiological phenomena.

Daniela O. H. Suzuki (M'09) received a graduate degree in Electrical Engineering in 1996 and a Ph.D. degree in Electrical Engineering in 2009 from the Federal University of Santa Catarina (UFSC), Florianópolis-SC, Brazil. She is currently an Assistant Professor at the Federal University of Santa Catarina. Her current interests include modeling biological processes, experimental and numerical investigation of membrane electropermeabilization.